

Interaction between longitudinal rolls and transverse waves
in unstably stratified plane Poiseuille flow

by

K. FUJIMURA 藤村 薫 (原研)

Japan Atomic Energy Research Institute
Tokai-mura, Ibaraki 319-11

and

R.E. KELLY ロバート・ケリー (UCLA)

Mechanical, Aerospace and Nuclear Engineering Department
University of California
Los Angeles, CA 90024-1597

I. INTRODUCTION

A superimposed through flow in Rayleigh-Bénard convection exerts a pattern selection mechanism that the convection roll is forced to be aligned in a longitudinal direction, i.e., parallel to the flow direction, if the flow field has an infinite extent. A longitudinal roll sets in for $Ra > Ra_c(Re)$ where Ra is the Rayleigh number and Ra_c denotes the critical Rayleigh number latter of which is a function of the Reynolds number, Re . Imagine that the through flow has a finite critical Reynolds number as is the case in plane Poiseuille flow. The longitudinal roll can then be critical for $0 \leq Re < Re_{LT}^*$ whereas a transverse traveling-wave, which is uniform in the direction perpendicular to the flow, becomes the critical mode for $Re > Re_{LT}^*$ as was clarified by Gage & Reid.¹ Here we denote Re_{LT}^* as a cross-over Reynolds number between the critical longitudinal roll and the critical transverse traveling-wave. It is thus natural to expect that a longitudinal roll interacts with a transverse traveling-wave, non-resonantly, in the neighborhood of the cross-over point, $(Ra, Re) = (Ra^*, Re_{LT}^*)$.

Nonlinear interactions between longitudinal rolls and transverse modes have recently been analyzed in thermal convection systems with mean shears: Rayleigh-Bénard convection in plane Couette flow,² Rayleigh-Bénard convection in plane Poiseuille flow with an existence of side walls,^{3,4} heated concentric annuli with rotation,⁵ and an inclined heated slot.⁶ In refs.3,5, and 6, non-resonant cubic amplitude equations predict an existence of a stable mixed mode composed of a longitudinal component and a transverse component. Moreover, in refs.5 and 6, the mixed mode bifurcates from a subcritical region with respect to the longitudinal roll. These seem to be a common feature of the mode interaction between a supercritical transverse mode and a supercritical longitudinal mode. But very recently, the mixed mode solution in Rayleigh-Bénard convection with plane Poiseuille flow was shown to be unstable in ref.4.

Let us concentrate our attention on the Rayleigh-Bénard convection in plane Poiseuille flow. Brand et al.³ considered an interaction between a transverse roll and a longitudinal roll in the convection with *weak* through flow under an existence of side walls. The existence

forces the transverse roll be the critical for small Reynolds number, $0 \leq Re \leq Re_{TL}^*$ say, while a longitudinal roll becomes critical if Re exceeds Re_{TL}^* where Re_{TL}^* denotes another cross-over Reynolds number between the transverse roll and the longitudinal one. According to Platten & Legros,⁷ $Re_{TL}^* \sim 10$ or less for $1 \leq P \leq 453$ and for two aspect ratios, 2 and 5.2. Brand et al.³ assumed a smallness of Re_{TL}^* and introduced coupled Ginzburg-Landau equations as model which describes the spatio-temporal evolution of disturbance amplitudes in the neighborhood of $(Ra, Re) = (Ra^*, Re_{TL}^*)$. They showed the existence of a stable mixed mode and also demonstrated how two modes switches with each other spatio-temporally as an initial value problem. Müller et al.⁴ re-examined the same problem but with more rational fashion. They derived coupled Ginzburg-Landau equations on a weakly nonlinear basis under a strong assumption about the side-wall effects and concluded that the mixed mode solution is unstable. They also demonstrated spatio-temporal evolution of both modes.

In the present paper, we consider a case that the Rayleigh-Bénard convection with plane Poiseuille flow is in two horizontal plates with infinite extent. In the case of the interaction between a longitudinal roll and a transverse traveling-wave in the neighborhood of $(Ra, Re) = (Ra^*, Re_{LT}^*)$, the cross-over Reynolds number Re_{LT}^* is large enough, i.e., $5490 < Re_{LT}^* < Re_c = 5772.2218$ for $P \geq 0.001$. The traveling wave should therefore be regarded as the Tollmien-Schlichting wave so that the wave itself exhibits a subcritical feature. An interaction between the transverse traveling-wave and a longitudinal roll is expected to yield quite different bifurcation characteristics from what have been obtained in the previous investigations on supercritical/supercritical mode interactions.

The objective of the present paper is to clarify bifurcation characteristics which arise in mode interactions between a supercritical longitudinal roll and a subcritical transverse traveling-wave. Our approach to investigate is on a weakly nonlinear basis which is consistent with fluid dynamics equations up to the cubic order approximation. Amplitude equations obtained on this basis cannot predict any existence of stable equilibrium periodic solutions for subcritical Hopf bifurcations. Note however that the local bifurcation characteristic in the isothermal plane Poiseuille flow helped us substantially to understand transition processes in shear flows. The local bifurcation characteristics obtained in the present paper should therefore provide us physically as well as mathematically important and interesting informations as we will see later.

After deriving nonlinear disturbance equations in §2, we reduce the nonlinear disturbance equations to two coupled amplitude equations on a weakly nonlinear basis in §3, and examine their bifurcation characteristics in §4.

II. MATHEMATICAL FORMULATION

Consider two horizontal parallel plates with infinite extent located at $z^* = \pm H$. Temperatures on the lower plate and the upper plate are maintained at $T_0 + \Delta T$ and $T_0 - \Delta T$, respectively, where T_0 and ΔT are positive constants. We impose a pressure gradient in x -direction which drives the plane Poiseuille flow between the plates. Governing equations of momentum, energy, and continuity are

$$\rho \left[\frac{\partial \mathbf{v}^*}{\partial t^*} + (\mathbf{v}^* \cdot \nabla^*) \mathbf{v}^* \right] = -\nabla^* p^* - \rho g [1 - \alpha(T^* - T_0)] \bar{\mathbf{e}}_z^* + \mu \nabla^{*2} \mathbf{v}^*,$$

$$\begin{aligned} \frac{\partial T^*}{\partial t^*} + (\mathbf{v}^* \cdot \nabla^*) T^* &= \kappa \nabla^{*2} T^*, \\ \nabla^* \mathbf{v}^* &= 0, \end{aligned} \quad (2.1)$$

where ρ is the density, g is the acceleration due to gravity, α is the thermal expansion coefficient, μ is the viscous coefficient, κ is the thermal diffusivity, \mathbf{v}^* is the velocity vector, p^* is the pressure, and T^* is the temperature.

We nondimensionalize all the variables as usual: $(x^*, y^*, z^*) = (Hx, Hy, Hz)$, $\mathbf{v}^* = U_0 \mathbf{v}$, $t^* = Ht/U_0$, $T^* = \Delta T \cdot T$, and $p^* = \rho U_0^2 p$ where U_0 denotes the center velocity of the plane Poiseuille flow. We further split \mathbf{v} , p , and T into the basic state $(\bar{\mathbf{v}}, \bar{p}, \bar{T})$ and the disturbance $(\hat{\mathbf{v}}, \hat{p}, \hat{T})$. The basic state has the solution of the form of

$$\bar{\mathbf{v}} \equiv (\bar{u}, 0, 0) = (1 - z^2, 0, 0), \quad \bar{T} = -z. \quad (2.2)$$

Elimination of the pressure terms yields the final form of the disturbance equations

$$\begin{aligned} \partial_t(\hat{u}_y - \hat{v}_x) + \bar{u} \partial_x(\hat{u}_y - \hat{v}_x) + \bar{u}_z \hat{w}_y \\ &= Re^{-1} \nabla^2(\hat{u}_y - \hat{v}_x) - \partial_y(\hat{\mathbf{v}} \cdot \nabla) \hat{u} + \partial_x(\hat{\mathbf{v}} \cdot \nabla) \hat{v} \\ \partial_t \nabla^2 \hat{w} + \bar{u} \nabla^2 \hat{w}_x - \bar{u}_{zz} \hat{w}_x \\ &= Ra Re^{-2} P^{-1} \nabla^2 \hat{T} + Re^{-1} \nabla^4 \hat{w} \\ &\quad - \{ \nabla^2(\hat{\mathbf{v}} \cdot \nabla) \hat{w} - \partial_z[\partial_x(\hat{\mathbf{v}} \cdot \nabla) \hat{u} + \partial_y(\hat{\mathbf{v}} \cdot \nabla) \hat{v} + \partial_z(\hat{\mathbf{v}} \cdot \nabla) \hat{w}] \}, \\ \partial_t \hat{T} + \bar{u} \hat{T}_x + \bar{T}_z \hat{w} &= Re^{-1} P^{-1} \nabla^2 \hat{T} - (\hat{\mathbf{v}} \cdot \nabla) \hat{T}, \\ \hat{u}_x + \hat{v}_y + \hat{w}_z &= 0, \end{aligned} \quad (2.3)$$

where Ra is the Rayleigh number defined by $\alpha g \Delta T H^3 / \mu \kappa$, Re is the Reynolds number defined by $U_0 H \rho / \mu$, P is the Prandtl number defined by $\rho \kappa / \mu$, and suffices attached to the dependent variables denote the differentiation. Boundary conditions are imposed as

$$\hat{u} = \hat{v} = \hat{w} = \hat{w}_z = \hat{T} = 0 \quad \text{at } z = \pm 1. \quad (2.4)$$

III. WEAKLY NONLINEAR REDUCTION

We now derive coupled amplitude equations which govern the temporal evolution of complex amplitude functions for transverse traveling-waves and for longitudinal rolls in the neighborhood of the cross-over point.

Let

$$\begin{aligned} [\hat{u}, \hat{v}, \hat{w}, \hat{T}]^T &= (\epsilon \vec{\Psi}_1 + \epsilon^3 \vec{\Psi}_1^{(1)} + \dots) E_1 + (\epsilon \vec{\Psi}_2 + \epsilon^3 \vec{\Psi}_2^{(1)} + \dots) E_2 \\ &\quad + \epsilon^2 \sum_{m,n=-2} \vec{\Psi}_{mn} E_m E_n + h.o.t. + c.c. \end{aligned} \quad (3.1)$$

where $\epsilon^2 \equiv 1/Re_c - 1/Re$, $E_n \equiv \exp[i\alpha_n(x - c_n t) + i\beta_n y]$, and the suffices 1 and 2 respectively denote the transverse traveling-wave and the longitudinal roll. Therefore, $\alpha_2 = c_2 = \beta_1 = 0$. We also set $Ra - Ra_c \equiv \epsilon^2 \tilde{R}$ where $\tilde{R} \sim 1$.

For later convenience, we introduce the following linear operators :

$$L_{mn} = \begin{pmatrix} \beta_{mn}\mathcal{M}_{mn} & -\alpha_{mn}\mathcal{M}_{mn} & i\beta_{mn}\bar{u}_z & 0 \\ i\alpha_{mn} & i\beta_{mn} & \partial_z & 0 \\ 0 & 0 & \mathcal{L}_{mn} & RaRe^{-2}P^{-1}(\alpha_{mn}^2 + \beta_{mn}^2) \\ 0 & 0 & \bar{T}_z & -i(\alpha c)_{mn} + i\alpha_{mn}\bar{u} - Re^{-1}P^{-1}S_{mn} \end{pmatrix},$$

$$L_{mn,Re^{-1}} \equiv \frac{\partial L_{mn}}{\partial Re^{-1}}, \quad L_{mn,Ra} \equiv \frac{\partial L_{mn}}{\partial Ra}, \quad M_{mn} \equiv \begin{pmatrix} i\beta_{mn} & -i\alpha_{mn} & 0 & 0 \\ 0 & 0 & 0 & 0 \\ 0 & 0 & S_{mn} & 0 \\ 0 & 0 & 0 & 1 \end{pmatrix},$$

where

$$\begin{aligned} \mathcal{M}_{mn} &\equiv (\alpha c)_{mn} - \alpha_{mn}\bar{u} - iRe^{-1}S_{mn}, \\ \mathcal{L}_{mn} &\equiv -i(\alpha c)_{mn}S_{mn} + i\alpha_{mn}\bar{u}S_{mn} - i\alpha_{mn}\bar{u}_{zz} - Re^{-1}S_{mn}^2, \\ \alpha_{mn} &\equiv \alpha_m + \alpha_n + \dots, \quad \beta_{mn} \equiv \beta_m + \beta_n + \dots, \\ (\alpha c)_{mn} &\equiv \alpha_m c_m + \alpha_n c_n + \dots, \quad \text{and } S_{mn} \equiv \partial_{zz} - \alpha_{mn}^2 - \beta_{mn}^2. \end{aligned}$$

We apply the method of multiple scales by introducing

$$t_n \equiv \epsilon^{2n}t, \quad \partial/\partial t = \sum_{n=0} \epsilon^{2n} \partial/\partial t_n. \quad (3.2)$$

Substitution of (3.1) and (3.2) into (2.3) and equating coefficients of $\epsilon^j E_1^m E_2^n$ to zero, we obtain a system of equations for $\vec{\Psi}_{mn}^{(k)}$ as follows. At $O(\epsilon)$, linear equations

$$L_j \vec{\Psi}_j(t_1, t_2, \dots; z) = 0, \quad j = 1, 2, \quad (3.3)$$

are obtained. Because the operator L_j does not involve an explicit time dependence, the solution $\vec{\Psi}_j$ is expressed as $\vec{\Psi}_j = A_j(t_1, t_2, \dots)\vec{\Phi}_j(z)$ where A_j is a complex amplitude function whose evolution is governed by coupled amplitude equations derived just below.

At $O(\epsilon^2)$, we obtain equations for $\vec{\Psi}_{11}, \vec{\Psi}_{12}, \vec{\Psi}_{22}, \vec{\Psi}_{-11}, \vec{\Psi}_{-12}, \vec{\Psi}_{-22}$ whose solutions are expressed as $A_1^2 \vec{\Phi}_{11}(z), A_1 A_2 \vec{\Phi}_{12}(z), A_2^2 \vec{\Phi}_{22}(z), |A_1|^2 \vec{\Phi}_{-11}(z), \bar{A}_1 A_2 \vec{\Phi}_{-12}(z), |A_2|^2 \vec{\Phi}_{-22}(z)$, respectively.

Finally at $O(\epsilon^3)$, we obtain equations for the deformations of the fundamental modes caused by nonlinear interactions :

$$L_j \vec{\Psi}_j^{(1)} = -M_j \vec{\Phi}_j \frac{\partial A_j}{\partial t_1} + L_{j,Re^{-1}} \vec{\Phi}_j \cdot A_j - \tilde{R} L_{j,Ra} \vec{\Phi}_j \cdot A_j + A_j \sum_{k=1}^2 |A_k|^2 \vec{N}_{-kkj}, \quad (3.4)$$

where N_{-kkj} denotes the nonlinear term whose explicit form is not listed here. The solvability condition for $\vec{\Psi}_j^{(1)}$ yields coupled amplitude equations of the form of

$$\frac{dA_j}{dt_1} = \tilde{\lambda}_j A_j + \sum_{k=1}^2 \lambda_{-kkj} |A_k|^2 A_j, \quad j = 1, 2, \quad (3.5)$$

where

$$\begin{aligned}\tilde{\lambda}_j &\equiv \lambda_j^{(Re)} + \tilde{R}\lambda_j^{(Ra)} \equiv \langle L_{j, Re^{-1}}\tilde{\Phi}_j \rangle_j - \tilde{R}\langle L_{j, Ra}\tilde{\Phi}_j \rangle_j, \\ \lambda_{-kkj} &\equiv \langle \tilde{N}_{-kkj} \rangle_j, \\ \langle \tilde{Q}(z) \rangle_j &\equiv \int_{-1}^1 \tilde{\Phi}_j(z)\tilde{Q}(z)dz / \int_{-1}^1 \tilde{\Phi}_j M_j \tilde{\Phi}_j dz,\end{aligned}$$

for arbitrary function $Q(z)$. The adjoint function $\tilde{\Phi}_j(z) = [0, 0, \tilde{w}_j, \tilde{T}_j]^T$ is a solution of the adjoint equation

$$\begin{aligned}[-i\alpha_1(\bar{u} - c_1)S_1 + 2i\alpha_1\bar{u}_z d/dz - Re^{-1}S_1^2]\tilde{w}_1 + \bar{T}_z\tilde{T}_1 &= 0, \\ RaRe^{-2}P^{-1}\alpha_1^2\tilde{w}_1 + [i\alpha_1(\bar{u} - c_1) - Re^{-1}P^{-1}S_1]\tilde{T}_1 &= 0,\end{aligned}$$

for transverse traveling-waves while

$$-Re^{-1}S_2^2\tilde{w}_2 + \bar{T}_z\tilde{T}_2 = 0, \quad RaRe^{-2}P^{-1}\beta_2^2\tilde{w}_2 - Re^{-1}P^{-1}S_2\tilde{T}_2 = 0,$$

for longitudinal rolls. Both equations are subject to homogeneous boundary conditions.

Coefficients involved in (3.5) are evaluated numerically for some particular Prandtl numbers under a constant pressure gradient condition. Numerical accuracy becomes worse as the Prandtl number increases. No reliable numerical coefficient was obtained for $P \geq 1000$.

IV. BIFURCATION CHARACTERISTICS AND DISCUSSIONS

In what follows, we utilize the original time scale t instead of the slow ones, t_n , $n \geq 1$ for simplicity. If we set $\epsilon A_j = a(j)e^{i\theta_j(t)}$ and $\epsilon^2 \tilde{\lambda}_j = \lambda_j$, the amplitude equation (3.5) for A_1 and A_2 are written in the form of

$$\begin{aligned}da_1/dt &= a_1(\lambda_{1r} + \lambda_{-111r}a_1^2 + \lambda_{-221r}a_2^2), \\ da_2/dt &= a_2(\lambda_2 + \lambda_{-112}a_1^2 + \lambda_{-222}a_2^2), \\ a_1 d\theta_1/dt &= a_1(\lambda_{1i} + \lambda_{-111i}a_1^2 + \lambda_{-221i}a_2^2),\end{aligned}\tag{4.1}$$

where subscripts r and i respectively denotes the real and the imaginary parts of the attached quantities. Equilibrium solutions of (4.1) are categorized as follows :

a) pure transverse traveling-wave (PT) :

$$a_1^2 = -\lambda_{1r}/\lambda_{-111r}, \quad a_2^2 = 0,\tag{4.2}$$

which is stable if $\lambda_{-111r} < 0$ and $\lambda_2 + \lambda_{-112}a_1^2 < 0$;

b) pure longitudinal roll (PL) :

$$a_1^2 = 0, \quad a_2^2 = -\lambda_2/\lambda_{-222},\tag{4.3}$$

which is stable if $\lambda_{-222} < 0$ and $\lambda_{1r} + \lambda_{-221r}a_2^2 < 0$;

c) mixed mode (M) :

$$a_1^2 = \frac{\lambda_2 \lambda_{-221r} - \lambda_{1r} \lambda_{-222}}{\lambda_{-111r} \lambda_{-222} - \lambda_{-112} \lambda_{221r}}, \quad a_2^2 = \frac{\lambda_{1r} \lambda_{-112} - \lambda_2 \lambda_{-111r}}{\lambda_{-111r} \lambda_{-222} - \lambda_{-112} \lambda_{-221r}}, \quad (4.4)$$

which is stable if

$$\text{Re} \left[a_1^2 \lambda_{-111r} + a_2^2 \lambda_{-222} \pm \sqrt{(a_1^2 \lambda_{-111r} + a_2^2 \lambda_{-222})^2 + 4a_1^2 a_2^2 (\lambda_{-221r} \lambda_{-112} - \lambda_{-111r} \lambda_{-222})} \right] < 0. \quad (4.5)$$

We show schematic bifurcation diagrams in $ReRa$ -plane in Fig.1 (a)-(c). Note that the range of validity of the present analysis is strictly limited in the neighborhood of the cross-over point $(Ra, Re) = (Ra^*, Re^*)$. In the figure, we exaggerated an existence region of each solution exceedingly so as to be able to find each sectors in $ReRa$ -plane, easily. Bifurcation diagrams are distinguished into three types depending on the value of the Prandtl number : $P \leq 0.44$, $0.45 \leq P \leq 4.6$, and $P \geq 4.7$. In each diagram, there are four or five boundaries of different solutions and different stability characteristics. These boundaries correspond to the linear critical curve for the transverse traveling-wave, the critical condition for the longitudinal roll ($Ra_c = 106.735111$), $a_1 = 0$ and $a_2 = 0$ in (4.4), i.e.,

$$\lambda_2 \lambda_{-221r} - \lambda_{1r} \lambda_{-222} = 0, \quad \text{and} \quad \lambda_{1r} \lambda_{-112} - \lambda_2 \lambda_{-111r} = 0,$$

and the stability boundary obtained from (4.5). The diagram for small P (Fig.1(a)) differs from the diagram for intermediate P (Fig.1(b)) only upon a stability characteristic of the mixed mode, M, while the diagram for intermediate P differs from the diagram for large P (Fig.1(c)) upon the existing region of the mixed mode. The different existing region of the mixed mode is due to a change of the sign of the denominator in (4.4) with the increase of P . The transverse traveling-wave has the subcritical feature. Indeed, λ_{-111r} is positive for all the values of the Prandtl number. In the case of the isothermal plane Poiseuille flow, the cubic order Landau equation predicts that the Tollmien-Schlichting wave bifurcates subcritically at the linear critical point and the unstable equilibrium amplitude is given by $\sqrt{-\lambda_{1r}(Re_c^{-1} - Re^{-1})/\lambda_{-111r}}$ whereas all the trajectories started from an initial condition except for exact zero blow up to infinity for $Re > Re_c$. In the present problem, the pure transverse traveling-wave solution and the mixed mode solution which is composed of the traveling wave component and the longitudinal one indeed exist as unstable equilibrium solutions in a subcritical state $Re < Re^*$. Remarkable and unexpected feature is, however, that a mixed mode solution exists stably in a supercritical state for the small and intermediate Prandtl number fluids, $P \leq 4.6$ (Fig.1 (a) and (b)), although the range of existence in $ReRa$ -plane is relatively narrow.

We show schematic trajectories in $a_1 a_2$ -plane as Fig.2 corresponding to each set of possible solutions and stability characteristics in Fig.1. In most of the cases, irrespective of the existence of stable equilibrium solutions, the amplitude equations (3.5) predict another trajectory, i.e., $a_1 \rightarrow \infty$ and $a_2 \rightarrow \infty$. This suggests an existence of another stable mixed mode solution with a large norm (hereafter referred to as M_∞). The M_∞ corresponds

to the two-dimensional stable equilibrium solution in an isothermal plane Poiseuille flow except for a region along the lower branch of the linear neutral stability curve. (Note also that there exists stable equilibrium solution bifurcates supercritically along the lower branch of the neutral stability curve.) Each $a_1 a_2$ -plane in Figs.2(a), (c), (e), (g), (h), (i), (j), and (l) is divided into two basins of attraction. The separator denoted by dashed curve can be determined only numerically.

We expect that the stable mixed mode, M, bifurcates from the stable pure longitudinal roll if the Reynolds number is gradually increased from zero while the Rayleigh number is fixed to be slightly greater than Ra^* . Otherwise, the mixed mode M never be achieved. Instead, any trajectory is attracted by another mixed mode with large norm, M_∞ .

In the present paper, we derived the amplitude equations (3.5) on the weakly nonlinear basis which is consistent with (2.3) up to the cubic order approximation. Even if we further proceed to higher order weakly nonlinear approximations, unfortunately, the above problems can never be resolved. Instead, we have to carry out a global analysis based upon full numerical method, eg., a continuation method based on the Euler-Newton method, to complete the bifurcation analysis for this physical setup. An evaluation of such global bifurcated solutions should be complementary to the present work and will form a future work.

REFERENCES

- ¹ K.S. Gage and W.H. Reid, "The stability of thermally stratified plane Poiseuille flow", *J. Fluid Mech.* **33**, 21 (1968).
- ² F.M. Richter, "Convection and the large-scale circulation of the mantle", *J. Geophys. Res.* **78**, 8735 (1973).
- ³ H.R. Brand, R.J. Deissler and G. Ahlers, "Simple model for the Bénard instability with horizontal flow near threshold", *Phys. Rev.* **A43**, 4262 (1991).
- ⁴ H.W. Müller, M. Tveitereid and S. Trainoff, "The Rayleigh-Benard problem with imposed weak throughflow : two coupled Ginzburg-Landau equations", to appear in *Phys. Rev.*
- ⁵ M. Kropp and F.H. Busse, "Secondary fluid flow in a rotating narrow cylindrical annulus heated from the side", *Phys. Fluids* **A3**, 2988 (1991).
- ⁶ K. Fujimura and R.E. Kelly, "Mixed mode convection in an inclined slot", *J. Fluid Mech.* **246**, 545, (1993).
- ⁷ J.K. Platten and J.C. Legros, "Convection in Liquids", (Springer, New York, 1984), p.559.

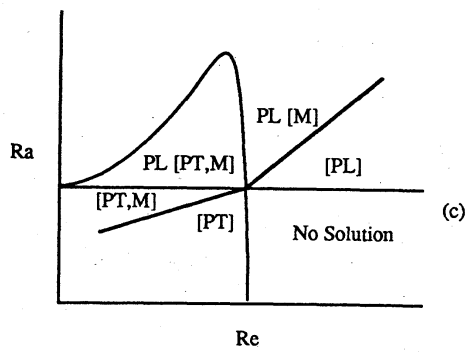
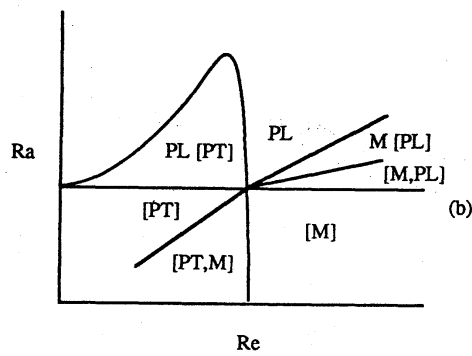
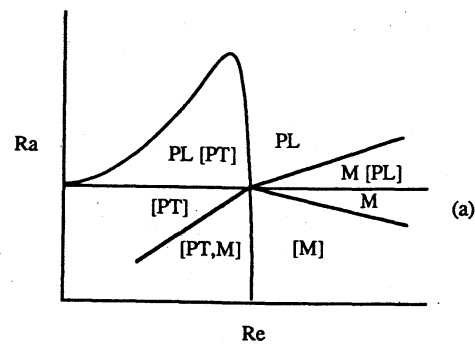


Fig.1 Schematic bifurcation diagrams. Letters without bracket denote stable equilibrium solutions while bracketed letters denote unstable equilibrium solutions. "No solution" denotes that there is no equilibrium solution irrespective of the stability characteristics. (a), $P \leq 0.44$; (b), $0.45 \leq P \leq 4.6$; (c), $P \geq 4.7$.

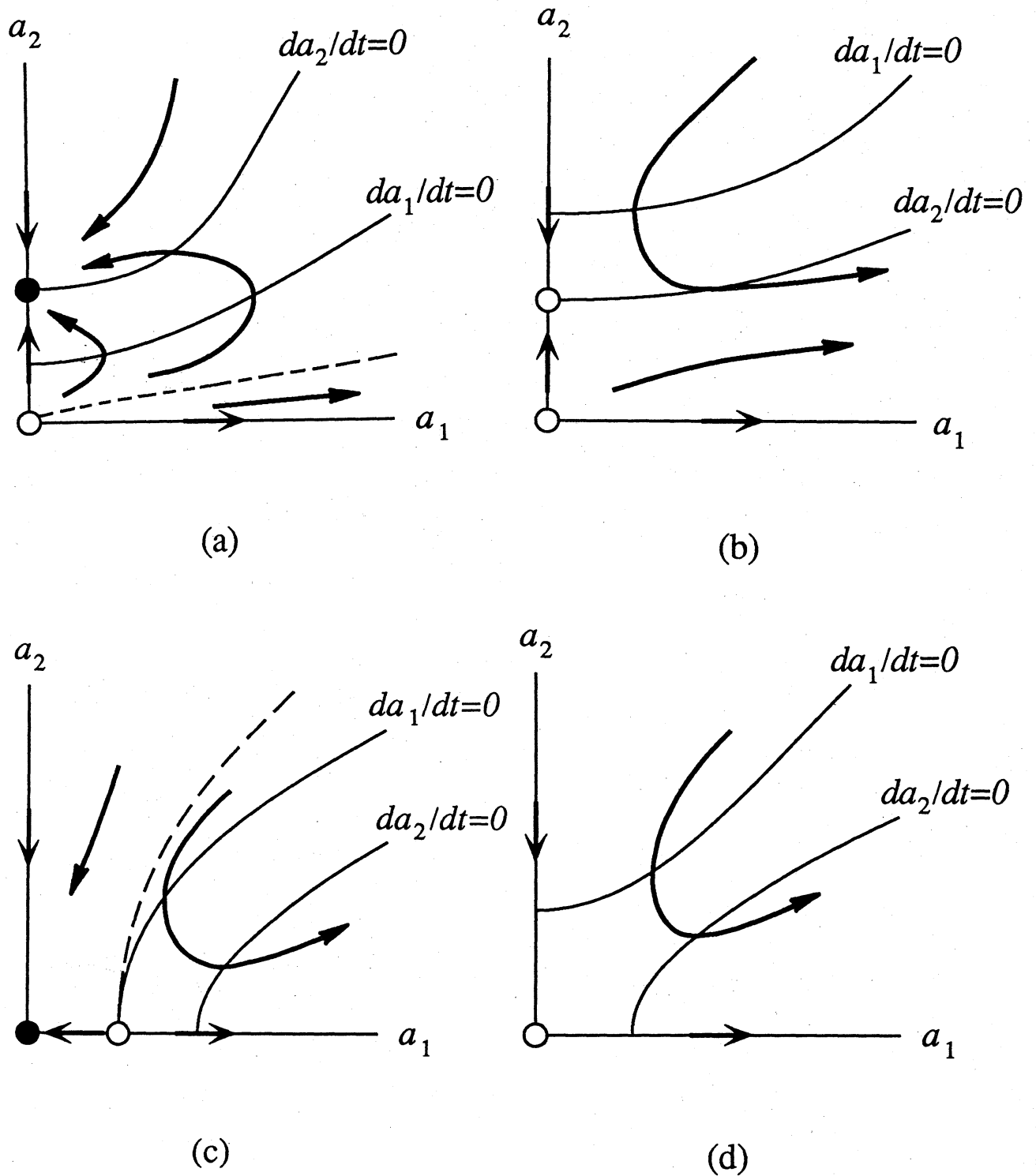
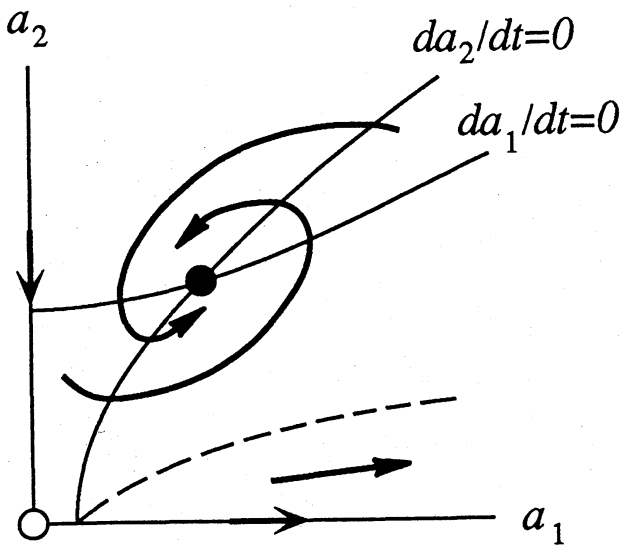
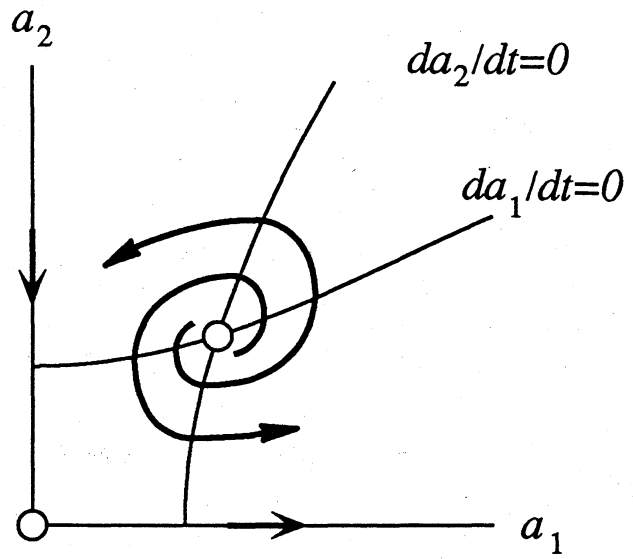


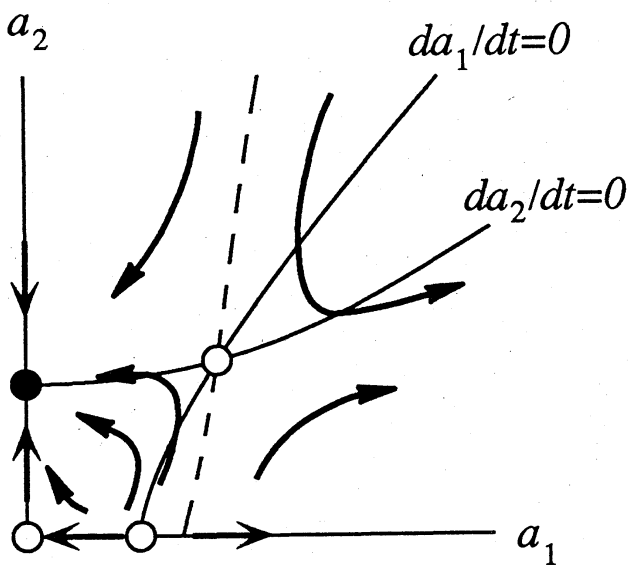
Fig.2 Schematic trajectories for each set of possible solutions and their stability characteristics in Fig.1. (a), PL ; (b), [PL] ; (c), [PT] ; (d), no solution ; (e), M ; (f), [M] ; (g), PL, [PT,M] ; (h), [PT,M] ; (i), M, [PL] ; (j), PL, [M] ; (k), [M,PL] ; (l), PL, [PT]. Open circles denote unstable equilibrium solutions while closed circles denote stable ones. Dashed curves denote separators dividing two basins of attraction.



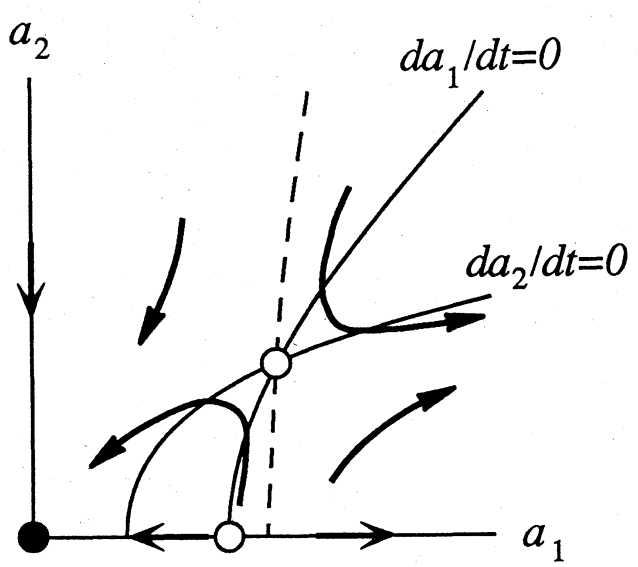
(e)



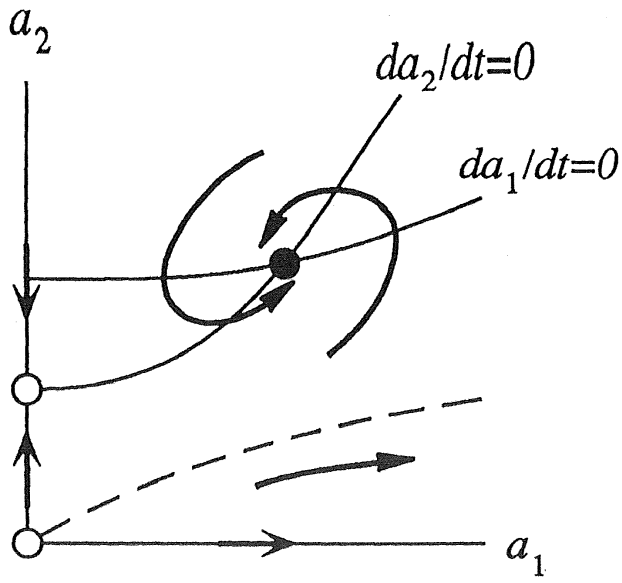
(f)



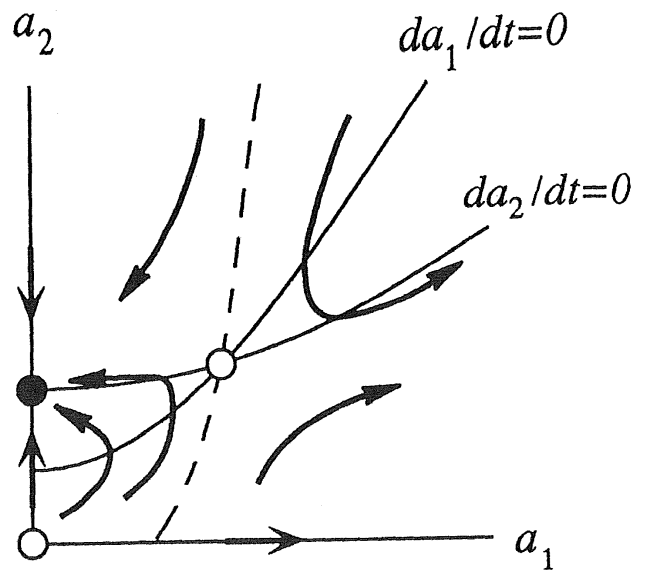
(g)



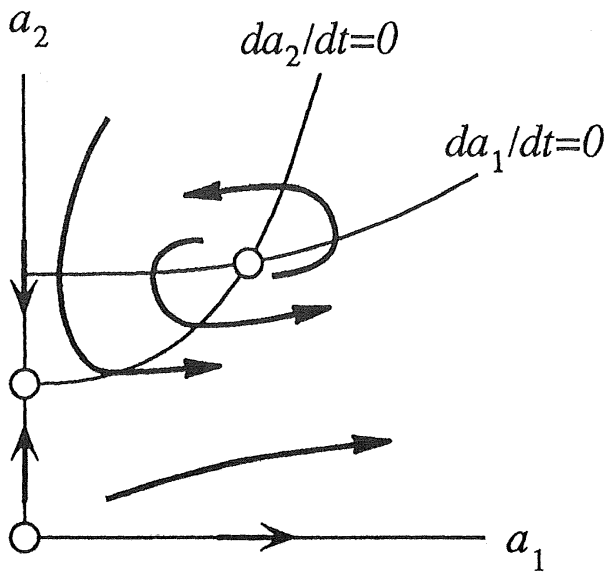
(h)



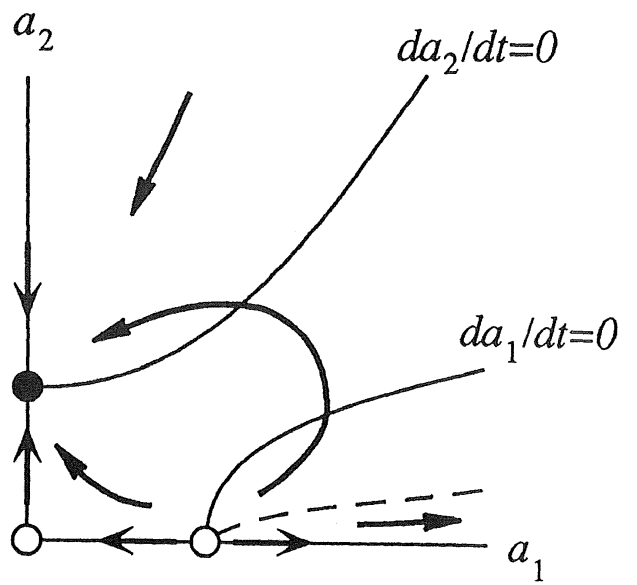
(i)



(j)



(k)



(l)